Trees
https://doi.org/10.1007/s00468-021-02114-x

ORIGINAL ARTICLE

Singlet oxygen, flavonols and photoinhibition in green and senescing silver birch leaves

Heta Mattila[1] · Pooneh Sotoudehnia[1] · Telma Kuuslampi[1] · Ralf Stracke[2] · Kumud B. Mishra[3] · Esa Tyystjärvi[1]

Received: 7 July 2020 / Accepted: 4 March 2021

Abstract

Key message **Decreased absorptance and increased singlet oxygen production may cause photoinhibition of both PSII and PSI in birch leaves during autumn senescence; however, photosynthetic electron transfer stays functional until late senescence.**

Abstract During autumn senescence, deciduous trees degrade chlorophyll and may synthesize flavonols. We measured photosynthetic parameters, epidermal flavonols, singlet oxygen production in vivo and photoinhibition of the photosystems (PSII and PSI) from green and senescing silver birch (*Betula pendula*) leaves. Chlorophyll *a* fluorescence and P_{700} absorbance measurements showed that the amounts of both photosystems decreased throughout autumn senescence, but the remaining PSII units stayed functional until ~ 90% of leaf chlorophyll was degraded. An increase in the chlorophyll *a* to *b* ratio, a decrease in > 700 nm absorbance and a blue shift of the PSI fluorescence peak at 77 K suggest that light-harvesting complex I was first degraded during senescence, followed by light-harvesting complex II and finally the photosystems. Senescing leaves produced more singlet oxygen than green leaves, possibly because low light absorption by senescing leaves allows high flux of incident light per photosystem. Senescing leaves also induced less non-photochemical quenching, which may contribute to increased singlet oxygen production. Faster photoinhibition of both photosystems in senescing than in green leaves, under high light, was most probably caused by low absorption of light and rapid singlet oxygen production. However, senescing leaves maintained the capacity to recover from photoinhibition of PSII. Amounts of epidermal flavonols and singlet oxygen correlated neither in green nor in senescing leaves of silver birch. Moreover, *Arabidopsis thaliana* mutants, incapable of synthesizing flavonols, were not more susceptible to photoinhibition of PSII or PSI than wild type plants; screening of chlorophyll absorption by flavonols was, however, small in *A. thaliana*. These results suggest that flavonols do not protect against photoinhibition or singlet oxygen production in chloroplasts.

Keywords Autumnal senescence · NPQ · Flavonoid · Oxidative stress · Photodamage · Photosynthesis · Reactive oxygen species

Introduction

During autumn senescence, deciduous trees degrade a vast number of macromolecules to remobilize nutrients for winter storage. Among the degraded complexes are chlorophyll-binding proteins of photosynthetic electron transport chain, including photosystem II (PSII), photosystem I (PSI) and their light harvesting antennae (LHCII and LHCI). Unbound chlorophylls can cause trouble since under illumination they would produce the harmful singlet oxygen ($^1O_2$; for reviews, see Mattila et al. 2015; Di Mascio et al. 2019). Indeed, accumulation of intermediates of chlorophyll degradation or biosynthesis has been shown to lead to massive $^1O_2$ production, oxidative damage and, finally, cell death in mutant plants

Communicated by Heckathorn .

✉ Esa Tyystjärvi
esatyy@utu.fi

[1] Molecular Plant Biology, University of Turku, Turku, Finland

[2] Genetics and Genomics of Plants, Bielefeld University, Bielefeld, Germany

[3] Global Change Research Institute, Czech Academy of Sciences, Bělidla 986/4a, 603 00 Brno, Czech Republic

Published online: 16 March 2021

(Tanaka et al. 2003; Przybyla et al. 2008). $^1O_2$ production is known to initiate also signaling pathways leading to cell death (Przybyla et al. 2008). Consequently, even though the nitrogen atoms of the chlorophyll molecules are not remobilized (Kräutler et al. 1991; Curty and Engel 1996; for a review see Kuai et al. 2018), chlorophyll is degraded via controlled pathways to colorless end products which remain in the vacuole (Matile et al. 1988) and do not produce $^1O_2$ (Hörtensteiner 2004; Kashiyama and Tamiaki 2014; Kuai et al. 2018).

To our knowledge, it is not known whether $^1O_2$ production increases in deciduous species during autumn senescence. Varying results have been previously obtained with senescing *Hordeum vulgare* (barley). Only a small increase in $^1O_2$ production during dark-induced senescence has been observed in vivo (Springer et al. 2015), and no increase in $^1O_2$ production was observed in thylakoid membranes (normalized to chlorophyll content) isolated during developmental senescence (i.e. senescence of older leaves) from *H. vulgare* leaves (Jajić et al. 2015). Similarly, no increase in $^1O_2$ production by isolated thylakoids was observed during monocarpic (i.e. death of the whole plant when seeds develop) senescence (Krieger-Liszkay et al. 2015). On the contrary, large amounts of $^1O_2$ were produced during methyl jasmonate-induced senescence (Springer et al. 2015) and during monocarpic senescence in another *H. vulgare* accession (Lomerit; Krieger-Liszkay et al. 2015). Krieger-Liszkay et al. (2015) showed that the Lomerit accession degraded PSII early during senescence and the authors concluded that the degradation of PSII or LHCII might be responsible for the observed $^1O_2$ production.

The order in which the components of the photosynthetic electron transport chain are degraded upon senescence varies according to species and may differ even between varieties of a species (Krieger-Liszkay et al. 2015). For example, in *Acer saccharum* (sugar maple) PSI and LHCI are degraded early, but in *Quercus bicolor* (swamp white oak) both photosystems are degraded before LHCs (Moy et al. 2015). In general, fates of photosynthetic components during autumn senescence in deciduous trees are not well understood. LHCI contains only little chlorophyll *b* and the cores of PSII and PSI none (Mazor et al. 2015; Wei et al. 2016); therefore changes in the chlorophyll *a* to *b* ratio offer information about the order in which the complexes are degraded. In tree species, the ratio commonly decreases during (autumn) senescence, e.g. in *Betula populifolia* (grey birch), *Q. bicolor* and *A. saccharum* (Lee et al. 2003; Moy et al. 2015). However, even though the components of the photosynthetic electron transport chain are degraded, the chain may remain remarkably functional until late senescence (Keskitalo et al. 2005; Kotakis et al. 2014; Moy et al. 2015; Mattila et al. 2018). It has been argued that keeping photosynthesis functional as long as possible ensures efficient nutrient resorption (Keskitalo et al. 2005; Moy et al. 2015). Accordingly, Hoch et al. (2003) found that increased PSII damage and chlorophyll degradation under high light and low temperature coincided with less efficient nutrient removal during senescence in anthocyanin-deficient mutants of *Cornus sericea* (red osier), *Vaccinium elliottii* (Elliott's blueberry), and *Viburnum sargentii*.

Asymmetric degradation of components of (photosynthetic) electron transport chain in senescing leaves may lead to the production of $^1O_2$ and also other reactive oxygen species (ROS; Krieger-Liszkay et al. 2019). Indeed, the amounts of ROS, mainly hydrogen peroxide, have been observed to increase during (or prior to) visual senescence, simultaneously with cellular damage (Dhindsa et al. 1981), also in some deciduous trees (Cheeseman 2009; Shi et al. 2012). Levels of any ROS depend not only on the rates of its production but also on the rates of detoxification. The detoxification mechanisms often decline during senescence (Procházková and Wilhelmová 2007). For example, activities of catalase and ascorbate peroxidase decrease in some deciduous trees throughout autumn senescence (Kukavica and Jovanovic 2004). However, enhancements of antioxidative systems during senescence have also been reported; for example, in *B. pendula* (silver birch) transcription of many genes encoding proteins with antioxidative functions, e.g. ascorbate peroxidase, increases during senescence (Sillanpää et al. 2005). ROS also function as signaling molecules, and an increase in (chloroplast-derived) ROS has been proposed to act as a signal initiating senescence (Leshem 1988; Hung and Kao 2005; Wang et al. 2016; Mayta et al. 2018).

The amounts of flavonoids, especially those of anthocyanins, often increase during senescence (Lee et al. 2003). It has been suggested that these secondary metabolites can act as screens for visible light and/or ultraviolet (UV) radiation. Anthocyanins may also function as antioxidants as they can quench $^1O_2$ (Csepregi and Hideg 2017). Hoch et al. (2003) showed that anthocyanin-deficient mutants of several deciduous woody species can cope with optimal conditions but are damaged when exposed to high light stress at a low temperature. Birches (*Betula* spp.) usually do not synthesize large amounts of anthocyanins during senescence (Taulavuori et al. 2011); however, *B. papyrifera* (paper birch) was as tolerant against the stress conditions as species that accumulate anthocyanins (Hoch et al. 2003). An increase (up to 30%) in flavonols was observed to occur simultaneously with, or slightly after, the initiation of chlorophyll degradation during autumn senescence in *B. pendula* (Mattila et al. 2018). On the contrary, leaves that are fallen off contain smaller amounts of at least some flavonol species than green leaves in *B. pendula* (Paaso et al. 2017). In anthocyanin producing species, amounts of flavonols may either decrease (Sitko et al. 2019), increase or stay constant (Mattila et al. 2018) during senescence. Flavonol amount

has been shown to increase in response to UV radiation in *B. pendula* (Morales et al. 2010) and in response to coldness in *B. nana* (dwarf birch; Stark et al. 2015). Flavonols can react with $^1O_2$ and hydrogen peroxide (Majer et al. 2014; Csepregi and Hideg 2017), and the scavenging of hydrogen peroxide may have regulatory functions (An et al. 2016; Watkins et al. 2017; Muhlemann et al. 2018). However, the functional roles of flavonols in senescence are poorly understood.

B. pendula is an ecologically and economically important deciduous tree species endemic to north and central Eurasia (Hynynen et al. 2010). In this species, the fates of photosynthetic complexes during senescence have been little studied. Therefore, we aimed at better understanding if (and how) senescing leaves, while degrading chlorophyll and photosynthetic complexes, are able to cope with light-induced damage. We also tested whether the increase in flavonols, observed in *B. pendula* during senescence, protects chloroplast functions. Therefore, photoinhibition, electron transfer reactions, $^1O_2$ production in vivo and flavonols were measured during natural autumn senescence of *B. pendula*. It was found that even though both photosystems are prone to light-induced damage in senescing leaves, photosynthetic electron transfer stays functional and the leaves possess capacity to recover from the damage until almost all chlorophyll is degraded. Flavonols increase in senescing birch leaves, however, these flavonoid species do not seem to protect chloroplasts from photoinhibition.

Materials and methods

Plant material and growth conditions

Leaves were collected from three mature *B. pendula* Roth. trees, growing in a small park between a road and a forest (60°27′30.6"N 22°18′33.3"E, Turku, Finland; Fig. 1). Leaves were kept on moist paper in darkness before measurements (conducted on the same day as collection, unless otherwise indicated). *Arabidopsis thaliana* (L.) Heynh. wild type (Col-0 and Nö-0) and mutants (*fls1-2* and *ldox fls1-2*; RIKEN_PST16145 and SALK_028793 x RIKEN_PST16145, respectively; Stracke et al. 2009) were grown in a growth chamber (Weiss Gallenkamp) at the photosynthetic photon flux density (PPFD) of 150 µmol m^{-2} s^{-1} at 22 °C in 8 h/16 h day/night rhythm. After 4 weeks of growth, the growth light was supplemented with 5 W m^{-2} of UV-A (368 nm, ~ 15 nm full width at half maximum (FWHM); LED Fedy, Shenzen, China) for two weeks and then additionally for one week with 10 W m^{-2} of UV-A, to induce flavonol synthesis.

Pigment analyses

Chlorophylls were measured either after extraction in dimethylformamide (DMF) or non-invasively by an optical method (Dualex Scientific, Force-A, Paris, France; Cerovic et al. 2012). For the former, leaf discs ($d = 6$ mm) were incubated in DMF for three to seven days at 4 °C in darkness after which chlorophylls *a* and *b* were quantified spectrophotometrically according to the coefficients in Porra et al. (1989). Relative chlorophyll values recorded by Dualex were converted to µg cm^{-2} according to a previously established calibration curve (Mattila et al. 2018): Chlorophylls $a+b$ (µg cm^{-2}) = 1.1432 × Dualex—5.7427.

Flavonols were probed by measuring the ratio of chlorophyll *a* fluorescence induced by UV radiation to fluorescence induced by visible light from intact leaves either with Dualex (Force-A) or with a QEPro spectrometer (Ocean Optics). The method is based on absorption of UV radiation by flavonols. Thus, the presence of flavonols lowers chlorophyll excitation under a source of UV radiation, thereby decreasing fluorescence emission (Goulas et al. 2004). Flavonols do not absorb visible light, which allows visible-light-excited chlorophyll *a* fluorescence to be used for normalization of the results. When the QEPro spectrometer was used, leaves were illuminated with 368 nm UV-A radiation (LED Fedy; narrowed using 360 and 370 nm filters; Corion line filter, FWHM 10 nm; Newport Corp.) or 600 nm visible light (obtained through a Corion line filter, FWHM 10 nm; Newport Corp.) and chlorophyll fluorescence was recorded at 660–700 nm. Intensities of the 368 nm and 600 nm light were set low enough to prevent an actinic effect on chlorophyll *a* fluorescence yield. Dualex measures flavonols with a similar principle (Cerovic et al. 2012).

Pigment measurements were conducted in the laboratory, under dim light, except when chlorophyll and flavonol contents of single leaves were followed during autumn (between 27 August and 26 October 2018) in which case the measurements were conducted under field conditions, as described previously (Mattila et al. 2018).

Fluorescence, absorbance and photoinhibition

Unless otherwise indicated, chlorophyll *a* fluorescence and near-infrared (NIR) absorbance changes (reflecting the reduction state of P_{700}) were measured from excised leaves of *B. pendula* (collected between 30 August and 16 October 2019) or mutant and wild type *A. thaliana* with Dual/KLAS-NIR fluorometer/spectrophotometer (Walz GmbH; Schreiber and Klughammer 2016) as follows. A leaf, dark-acclimated for at least 30 min, was placed between the measuring heads of Dual/KLAS-NIR after which an automatic calibration was done. Actual measurements started with a 30 s dark incubation (only the measuring beam of

Fig. 1 A *B. pendula* tree during autumn 2018. The circles highlight the course of senescence in three individual leaves, marked with differently dashed circles. Between 18 and 22 October 2018, one of the leaves has fallen off. The last photograph shows senescing leaves with PSII yield (F_V/F_M) of 0.42 ± 0.02, collected from a different *B. pendula* tree

the fluorometer was on), after which a saturating pulse (SP; 800 ms) was fired to calculate $(F_M\text{-}F_O)/F_M = F_V/F_M$. After another 30 s, far-red (FR) light (735 nm, ~ 14 nm FWHM, set to maximum intensity) was switched on for 15 s, at the end of which a second SP was fired (to calculate the maximum amount of oxidizable P_{700}). In some cases, as indicated, a 45 s dark period followed, after which an actinic light was switched on for 2.5 min (621 nm, ~ 14 nm FWHM, PPFD 1650 µmol m^{-2} s^{-1}) or for 5 min (PPFD 1750 µmol m^{-2} s^{-1}; leaves collected 28 September 2020). An SP was fired every 60 s, during the actinic light and subsequent 2.5-min or 4.5-min darkness, to calculate non-photochemical quenching (NPQ; F_M/F_M'-1).

To induce photoinhibition, leaves were placed on a moist paper (temperature was set at 20 °C) and illuminated with a sunlight simulator (SLHolland; PPFD 2000 µmol m^{-2} s^{-1}).

F_V/F_M and P_{700} signals were recorded as described above. To test the recovery capacity, birch leaves were illuminated for 90 min (green leaves) or 30 min (senescing leaves) with the SLHolland sunlight simulator (PPFD 3000 µmol m^{-2} s^{-1}) and then allowed to recover for 11 h in low light (PPFD 20 µmol m^{-2} s^{-1}) at room temperature (~22 °C) with petioles in water. In the case of the recovery measurements, F_V/F_M was measured with FluorPen (Photon Systems Instruments, Czech Republic).

Leaf absorption spectra

Absorption spectra were measured from nine leaf discs ($d = 9$ mm), obtained from at least three leaves of *B. pendula* (collected on 1 October 2019) using an integrating sphere (Labsphere). A slide projector was used for illumination and spectra were measured with a calibrated STS-VIS spectrometer (Ocean Optics). Absorption of the sphere itself was calibrated according to Idle and Proctor (1983) by measurements with matt black cardboard earlier calibrated for reflectance (Pätsikkä et al. 1998). The measurement was done to obtain the relative difference between yellow and green leaves and full quantitation of the absorptance was not attempted.

Singlet oxygen measurement

Leaf discs ($d = 6$ mm) of *B. pendula* (collected between 4 and 5 October 2018) were vacuum infiltrated and incubated over-night in darkness in a solution containing 200 µM Singlet Oxygen Sensor Green (SOSG; Invitrogen™) and 4% methanol. Leaf discs were kept in water to prevent drying and illuminated (PPFD 2000 µmol m^{-2} s^{-1}) at 20 °C. Red light (> 650 nm) was used to prevent $^1O_2$ production by the sensor itself (Ragás et al. 2009). SOSG fluorescence was excited with 500 nm light (obtained through a Corion line filter, FWHM 10 nm), measured with a QEPro spectrometer (Ocean Optics) and quantified by integrating the signal at 530–535 nm. In $^1O_2$ measurements, F_V/F_M was measured with FluorPen (Photon Systems Instrument).

Estimation of the effect of leaf chlorophyll content on SOSG fluorescence

The effect of absorption of the leaf on SOSG fluorescence was estimated by assuming that a leaf is a homogenous layer (thickness 1) of absorbing material. Now, light intensity within the leaf at depth x from the upper surface is, according to the Lambert–Beer law

$$I(x) = I_0 e^{-\varepsilon x}, \tag{1}$$

where ε is the extinction coefficient. For simplicity, a natural-logarithm-based ε is used. The intensity of SOSG fluorescence at depth x is the product of I_0 and the fluorescence yield of SOSG (ϕ). Estimates for the values of ε at the excitation and emission wavelengths (ε_x and ε_m, respectively), are obtained from measurements of leaf absorptance α by noting that at leaf thickness 1, $I = 1$—α, and therefore $\varepsilon = \ln(1/(1—\alpha))$.

At the surface, SOSG fluorescence originating at depth x has the intensity

$$F(x) = I_0 \emptyset I(x) e^{-\varepsilon_m x} = I_0 \emptyset e^{-\varepsilon_x x} e^{-\varepsilon_m x} = I_0 \emptyset e^{-x(\varepsilon_x + \varepsilon_m)} \tag{2}$$

Observable SOSG fluorescence (F_{obs}), as a fraction of SOSG fluorescence that would have been obtained without any attenuation by the leaf ($F_{zero} = \phi I_0$) is then

$$\frac{F_{obs}}{F_{zero}} = \int_0^1 e^{-x(\varepsilon_x + \varepsilon_m)} dx = \frac{1}{\varepsilon_x + \varepsilon_m}\left(1 - e^{-(\varepsilon_x + \varepsilon_m)}\right). \tag{3}$$

When the sum $\varepsilon_x + \varepsilon_m$ approaches zero, F_{obs} approaches $I_0\phi$. The SOSG emission intensity that would be obtained if the leaf did not absorb the excitation or emission wavelength, is equal to the experimentally observed intensity divided by the quantity in Eq. 3.

As only relative absorption spectra of yellow and green leaves were available, the spectra were normalized by setting the absorptance of the green leaves to 100% at 430 nm; earlier measurements from green leaves (Hogewoning et al. 2012; Mattila et al. 2020) show over 95% absorptance in this region.

77 K fluorescence emission spectra

Leaf discs ($d = 6$ mm) of *B. pendula* (collected on 13 November 2019 from different birch individuals than in other experiments; 60°27′02.9"N 22°17′36.6"E, Turku, Finland) were frozen and ground in liquid nitrogen in the presence of quartz grains to dilute the sample (Weis 1985). Fluorescence was excited with 440 nm light (obtained through a Corion line filter, FWHM 10 nm) and measured with a QEPro spectrometer (Ocean Optics) in liquid nitrogen.

Figures and statistics

Figures were prepared in SigmaPlot (Systat Software, Inc). Statistical differences were calculated in Excel (Microsoft) with Student's t test (2-tailed distribution): paired between time points (within the same leaf) and otherwise

heteroscedastic (between different leaves). Linear regression was calculated by fitting a line (least squares) to the data points in Excel.

Results

While maximum fluorescence decreased, PSII yield remained high in a senescing leaf until almost all chlorophyll was degraded

To study natural senescence in *B. pendula*, leaves were collected from three outside-grown mature trees (Turku, Finland; Fig. 1) during the autumns 2018, 2019 and 2020, and brought to laboratory for measurements. As earlier shown in Mattila et al. (2018), senescence is a very rapid process at the level of an individual birch leaf (Fig. 1).

To investigate the photosynthetic reactions during autumn senescence, especially the fates of both photosystems (PSII and PSI), chlorophyll *a* fluorescence parameters and P_{700} absorbance changes were simultaneously recorded with Dual/KLAS-NIR fluorometer/spectrophotometer from dark-acclimated leaves with different chlorophyll concentrations. The fluorescence parameter F_V/F_M is a measure of the maximum quantum yield of PSII photochemistry and F_M is the maximum fluorescence value, obtained when all PSII reaction centers are closed for photochemistry. P_{700} absorbance changes, in turn, show the light-dependent oxidation and electron-transfer-dependent re-reduction of P_{700}, the primary donor of PSI. The maximum fluorescence yield, F_M (mainly originating in PSII; Franck et al. 2002), declined with decreasing chlorophyll content of the leaves (Fig. 2a). On the contrary, F_V/F_M stayed high until about 90% of chlorophyll was degraded, after which F_V/F_M declined rapidly (Fig. 2a). The results indicate that even though the amount of PSII decreased in senescing leaves, the remaining PSII units remained functional. During the degradation of chlorophyll, the chlorophyll *a* to *b* ratio increased in a biphasic manner. The data suggest that the ratio first increased very slowly until ~ 75% of chlorophyll had been degraded; the R^2 value of the trend, highlighted with a regression line in Fig. 2a, is weak but statistically significant. After this first phase, the chlorophyll *a* to *b* ratio rapidly increased (Fig. 2a). In a *B. pendula* leaf, the sequence of events depicted in Fig. 2 takes about a week (Fig S1; Mattila et al. 2018).

From here on, most measurements were conducted only with green leaves (30–40 µg chlorophyll cm^{-2}) and yellow (senescing) leaves that still had high PSII activity (4–15 µg chlorophyll cm^{-2}). First, we measured the absorption spectra of the leaves by placing green or senescing leaves inside an integrating sphere and measuring how much they absorb diffuse light at each wavelength (Idle and Proctor 1983). Not surprisingly, senescing leaves absorbed less light, although

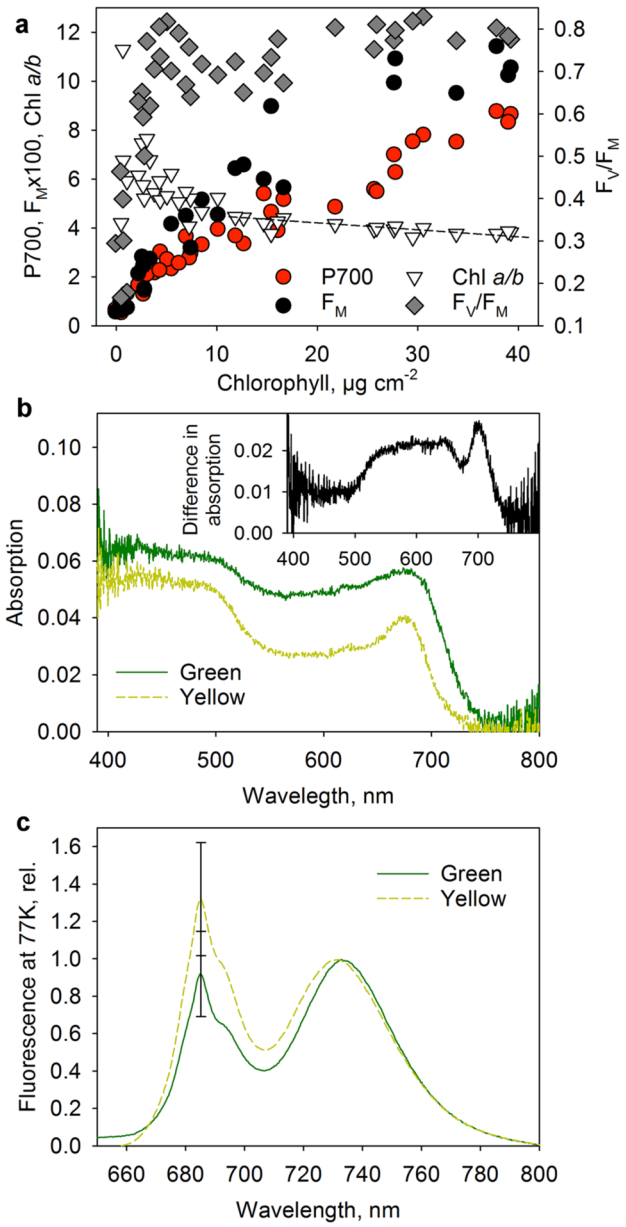

Fig. 2 Maximum quantum yield of PSII photochemistry (F_V/F_M), amount of oxidizable PSI (P_{700}), maximal fluorescence (F_M), chlorophyll (Chl) *a* to *b* ratio (a), in vivo absorption (b) and fluorescence spectra at 77 K (c), measured from *B. pendula* leaves with different chlorophyll concentrations. The dashed line in (**a**) is fitted to the chlorophyll *a/b* values with chlorophyll contents > 10 µg cm^{-2} (slope = -0.0238; $R^2 = 0.541$; $P = 0.0005$). The insert in (**b**) shows the difference in absorption between green and senescing leaves. The spectra in (**c**) are normalized to the peak value of PSI fluorescence. Chlorophyll ($a+b$) contents were 28.6 ± 2.44 and 4.85 ± 1.45 µg cm^{-2} in (**b**) and, before dilution, 12.6 ± 1.94 and 4.16 ± 0.88 µg cm^{-2} in (**c**), for green and senescing leaves, respectively. Chlorophyll was quantified spectrophotometrically after extraction with DMF. Values in (**a**) represent single measurements of leaves with different chlorophyll concentrations. Averages calculated from at least three biological replicates of green or senescing (yellow) leaves are shown in (**b**–**c**). Error bars show standard deviation (SD). Leaves in (**c**) were collected from different trees than leaves used in the rest of the experiments

the difference was proportionally smaller at wavelengths shorter than 500 nm than at other visible light wavelengths (Fig. 2b). The loss of absorbance was proportionally highest at the longest wavelengths absorbed by the leaves (insert in Fig. 2b).

Next, to specifically probe the fates of the two photosystems, we measured fluorescence spectra from diluted leaf powder at 77 K (Fig. 2c). Fluorescence spectra at 77 K, where contributions from different PSII and PSI related complexes to the emission spectrum are well resolved (see Wientjes et al. 2011), provides an estimate of the ratio of the number of chlorophyll molecules associated with PSII to those associated with PSI. Dilution of the leaf material by quartz sand (Weis 1985) allows elimination of self-absorption that would otherwise affect the ratio of the intensities of the spectral peaks. The data showed that the emission peak of PSI (~730 nm) was blue shifted by approximately 1 nm in senescing leaves. In addition, the ratio of PSII (~685 nm) to PSI fluorescence was higher in senescing leaves than in green ones (Fig. 2c). Leaves used for the 77 K measurements were collected from different *B. pendula* individuals than those used for all the other experiments, but the blue shift and the proportional decrease in the PSI fluorescence were consistently observed in five different individuals, suggesting that it is a general feature of *B. pendula* senescence.

Photosynthetic parameters in senescing and green leaves

To further compare the photosynthetic performance of leaves with different chlorophyll contents, chlorophyll *a* fluorescence transients and oxidation state of P_{700} were recorded during a light treatment and subsequent darkness (Fig. 3). Non-photochemical quenching (NPQ) and the coefficient of photochemical quenching (qL) during and after a 2.5 min high light illumination (PPFD 1650 µmol m^{-2} s^{-1}) were calculated from the fluorescence data. NPQ reflects the efficiency by which the photosynthetic machinery converts excitation energy to heat, and qL is a measure of the fraction of open PSII reaction centers (Kramer et al. 2004). Maximum fluorescence under light (F_M') was quenched to a greater degree, compared to dark-acclimated values (F_M), in green than senescing leaves, in line with higher NPQ levels in green leaves (Fig. 3a, c). Relaxation of NPQ after switching off the light was similar in both types of leaves (Fig. 3a, c). NPQ increased up to 4 or 5 min of illumination in both leaf types but yellow leaves always showed less NPQ than green ones (Fig. S2). On the contrary, there was no difference in qL between green and senescing leaves (Fig. 3a, e), indicating that the photosynthetic electron flow functioned well in yellow leaves. The chlorophyll *a* fluorescence level measured in the dark was higher in senescing leaves than in green ones (Fig. 3a, e), and senescent leaves showed a higher ratio of F_M to chlorophyll content than green leaves (Fig. S3).

Far-red (FR) light oxidized P700 more efficiently in green than in senescing leaves (Fig. 3b, d). Switching on the strong actinic light, on the contrary, rapidly oxidized P_{700} in senescing leaves (Fig. 3b, f). In green leaves, stable oxidation was reached only after ~30 s (Fig. 3b, f). In addition, P_{700} was reduced more slowly in darkness after FR light treatment or SP in senescing than in green leaves (Fig. 3b). The slow reduction of P_{700} after FR treatment and rapid oxidation of P_{700} under visible actinic light suggest that the flow of electrons from the plastoquinone pool to P_{700}^{+} is slower in senescing than in green leaves.

Photoinhibition proceeded rapidly in senescing leaves

As the NPQ measurements (Fig. 3c) implied that senescing leaves may not be protected against high light as efficiently as green leaves, we next exposed the leaves to photoinhibitory light. Green and senescing leaves of *B. pendula* were illuminated from the adaxial side with high light simulating sunlight (PPFD 2000 µmol m^{-2} s^{-1}) for 90 min at 20 °C (Fig. 4) and activities of PSII and PSI were measured. High light caused a decrease in F_V/F_M (measured on both sides of the leaves) and P_{700} signal (Fig. 4a–b), indicating that high light caused a decrease in the activities of PSII and PSI in both leaf types. Both (PSII and PSI) signals decreased faster in senescing leaves (57% and 24% loss of activity of PSII (adaxial side) and PSI, respectively) than in green leaves (25% and 9% loss of activity of PSII (adaxial side) and PSI, respectively).

Next, we measured if the leaves could recover from the PSII damage. Green leaves were illuminated, at PPFD 3000 µmol m^{-2} s^{-1} for 90 min, and senescing leaves for 30 min to inhibit a similar fraction of PSII units (Fig. 4c). The capacity to recover from PSII photoinhibition was very similar in both types of leaves (Fig. 4c). However, after 3 h and 11 h of recovery, sufficient fluorescence signal could no longer be recorded from ~50% of senescing leaves, possibly due to bleaching of chlorophyll.

Senescing leaves produced more singlet oxygen, and flavonols did not affect singlet oxygen production

To understand the reasons behind the susceptibility of senescing leaves to photoinhibition and to probe the possible protective role of flavonols, $^1O_2$ production under high light (>650 nm; PPFD 2000 µmol m^{-2} s^{-1}) was measured from green and senescing leaves, hand-picked so that they contained different levels of flavonols (Fig. 5). Flavonols absorb

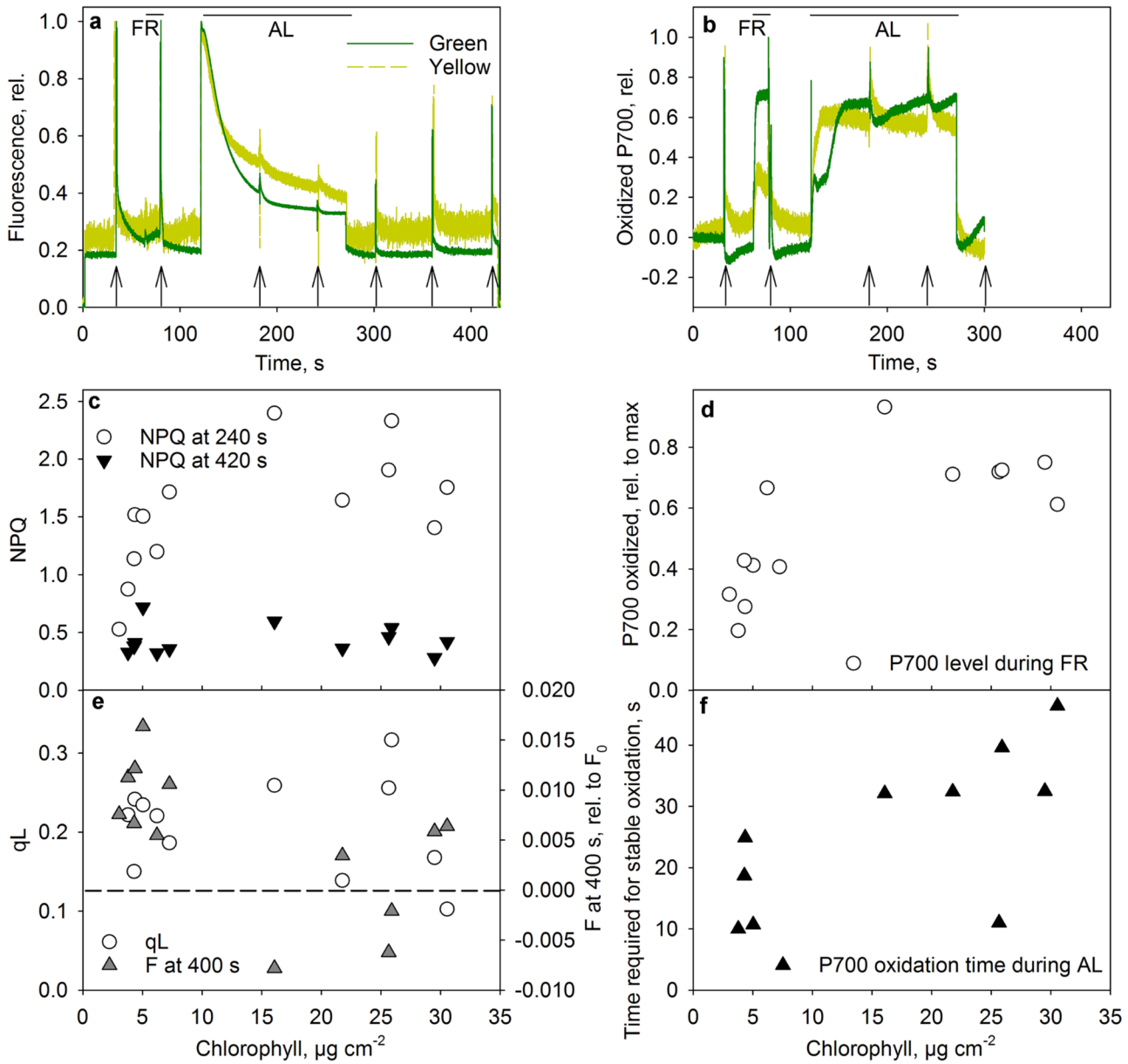

Fig. 3 Representative chlorophyll *a* fluorescence (**a**) and P_{700} (**b**) traces measured from dark-acclimated green and senescing (yellow) *B. pendula* leaves, treated with white saturating pulses (arrows), far-red (FR) and orange light (AL; PPFD 1650 µmol m^{-2} s^{-1}), at 20 °C. Chlorophyll (*a*+*b*) contents of green and senescing leaves were 30.6 and 4.46 µg cm^{-2}, respectively, in (**a**) and (**b**). Fluorescence curves are normalized to the maximum values, and P_{700} curves between the minimum and maximum values, and the green curve in (**b**) is additionally straightened between the start and end points to remove drift in the signal. Fluorescence (**c**, **e**) and P_{700} (**d**, **f**) parameters were measured from leaves with different chlorophyll contents, treated as shown in (**a**–**b**). Chlorophyll was quantified spectrophotometrically after extraction with DMF. Non-photochemical quenching of fluorescence (NPQ) was calculated as F_M/F_M'-1 and photochemical quenching of fluorescence (qL) as (F_M'-F)/(F_M'-F_0') x (F_0'/F) (fluorescence values at 275 s were taken as F_0'). F at 400 s indicates the difference in the fluorescence level in the darkness between the time points of 20 s and 400 s (**e**). P_{700} level during FR represents the amount of P_{700} oxidized during FR illumination relative to maximum oxidizable P_{700} (**d**); the time required for P_{700} to reach stable oxidation upon switching on AL is shown in (**f**)

UV radiation (see Csepregi and Hideg 2017) and, therefore, their amounts can be estimated by measuring the absorbance of UV radiation from intact leaves. In *B. pendula* the method works well; a difference in UV absorbance between yellow and green leaves seemed to be almost entirely due to increased flavonol content of the yellow leaves (measured by liquid chromatography; Mattila et al. 2018), presumably because birches do not accumulate much anthocyanins.

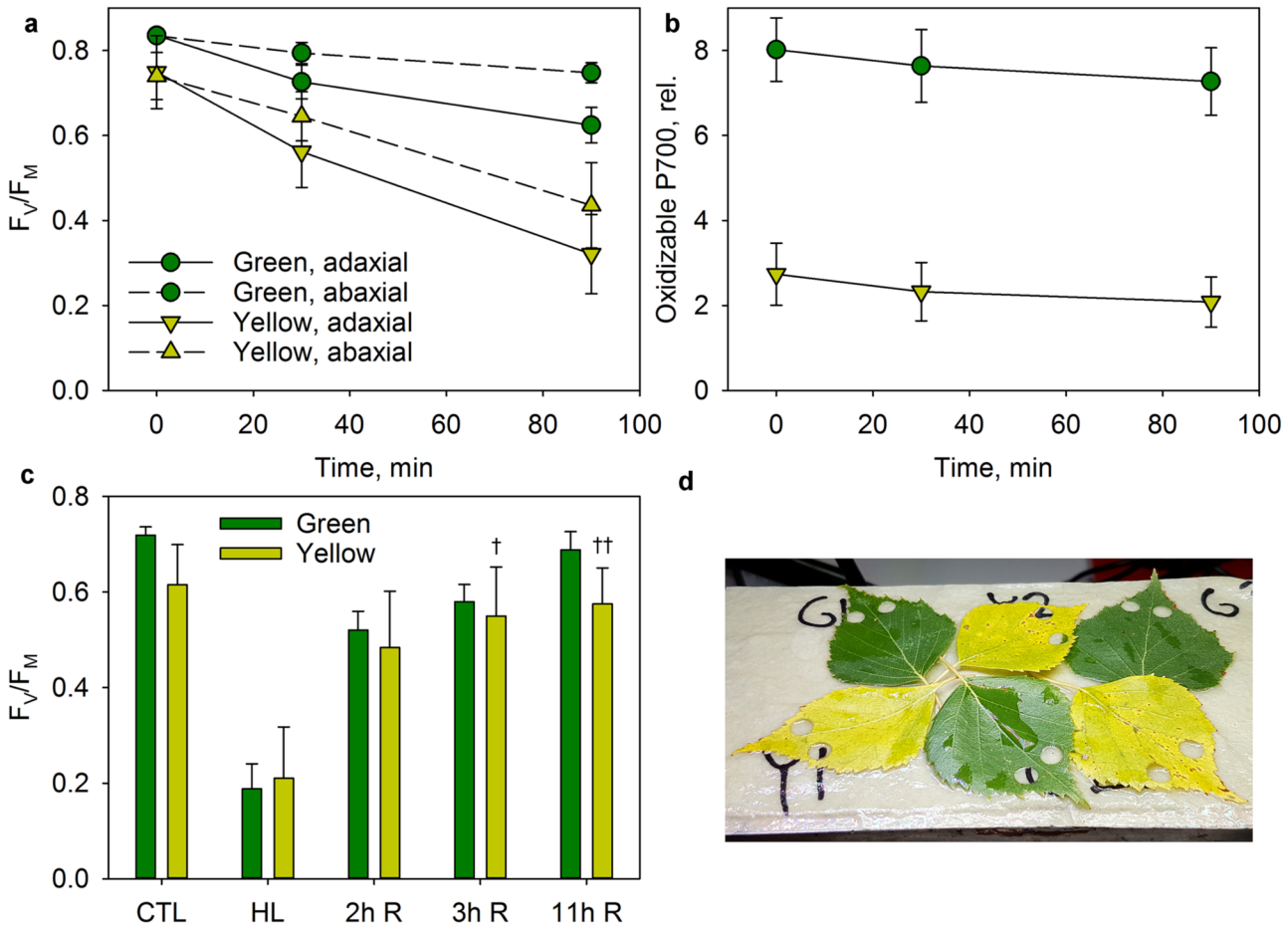

Fig. 4 Photoinhibition of PSII (**a**) and PSI (**b**) and recovery from PSII photoinhibition (**c**) in green and senescing (yellow) *B. pendula* leaves (**d**). F_V/F_M (**a**) was measured from the adaxial and abaxial sides of the leaf. Leaves were illuminated at the PPFD of 2000 (**a**–**b**) or 3000 µmol m^{-2} s^{-1} (HL; **c**) at 20 °C. In (**c**) green leaves were illuminated for 90 min and yellow leaves for 30 min. During subsequent recovery (R), leaves were illuminated with low light (PPFD 20 µmol m^{-2} s^{-1}). After 3 h of recovery, fluorescence signal could be detected from six out of seven senescing leaves (indicated by †) and after 11 h from four out of seven senescing leaves (††). Error bars show SD from three biological replicates. Initial chlorophyll ($a+b$) contents were 30.6 ± 6.3 and 5.12 ± 2.42 µg cm^{-2} in (**a**–**b**) and 18.1 ± 3.45 and 4.80 ± 1.92 µg cm^{-2} in (**c**), for green and senescing leaves, respectively. Chlorophyll was quantified spectrophotometrically after extraction with DMF

During autumn, the flavonol contents of individual leaves stayed constant, until an increase, coinciding with chlorophyll degradation, was observed (Fig. S1), in agreement with our previous study (Mattila et al. 2018). At the beginning of the autumn, however, different leaves of *B. pendula*, even from the same tree, contained different levels of flavonols (Fig. S1).

$^1O_2$ production was measured with the fluorescent dye SOSG; the fluorescence yield of the dye (at ~ 520–550 nm) increases upon reaction with $^1O_2$. All types of leaves produced $^1O_2$ during the 0–120 min illumination, but SOSG fluorescence increased during illumination significantly faster in senescing leaves than in green leaves (Fig. 5). The amount of flavonols, however, did not affect the rate of increase in SOSG fluorescence (Fig. 5). To estimate relative rates of $^1O_2$ production, between yellow and green leaves, the better penetration of both the 500 nm excitation light and 530–535 nm SOSG fluorescence in yellow than green leaves was taken into account. The effect of leaf chlorophyll concentration on the intensity of SOSG fluorescence was estimated according to Eq. 3 (see "Materials and methods"). As the leaf absorption spectra (Fig. 2b) had been measured only to obtain the difference in the spectral form, they were, therefore, normalized by assuming 100% absorptance for green leaves at 430 nm, which led to extinction coefficients $\varepsilon_x = 3.599$ and $\varepsilon_m = 1.821$ for green and $\varepsilon_x = 0.773$ and $\varepsilon_m = 1.611$ for yellow leaves, and thus the respective F_{obs}/F_{zero} values were 0.184 and 0.381 for green and yellow leaves. The slope of the increase in SOSG fluorescence, after the correction for leaf absorptance, was still 2.3–2.8 times as high in yellow than in green leaves, and the flavonoid content of the leaf did not affect the slope (Table S1). Thus,

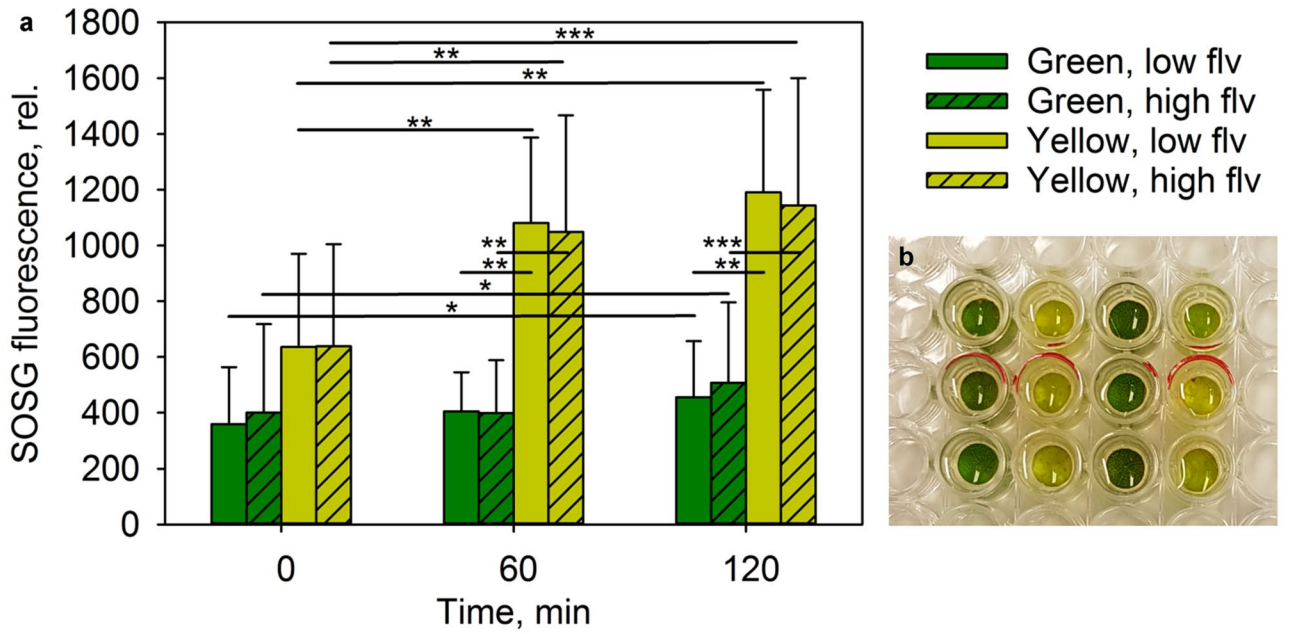

c

	Chlorophyll, µg cm^{-2}	Flv, arbitrary units	F_V/F_M
Green, low flv	29.0 (3.73)	1.24 (0.08)	0.79 (0.01)
Green, high flv	31.9 (2.28)	1.58 (0.09)	0.77 (0.03)
Yellow, low flv	10.5 (2.69)	1.27 (0.09)	0.77 (0.02)
Yellow, high flv	11.5 (3.69)	1.59 (0.11)	0.74 (0.04)

Fig. 5 Increase in SOSG fluorescence during high-light illumination of green and senescing (yellow) leaves of *B. pendula* with different flavonol (flv) contents (**a**). SOSG-infiltrated leaf discs (**b**) were illuminated for 0–120 min in high light (>650 nm; PPFD 2000 µmol m^{-2} s^{-1}), at 20 °C, and SOSG fluorescence at 530–535 nm was measured. Error bars show SD from six replicates. Statistically significant differences (Student's t-test; paired between time points, heteroscedastic otherwise) are indicated by * ($P<0.05$), ** ($P<0.01$) or *** ($P<0.001$). Averaged chlorophyll and flavonol contents (measured with an optical method) and PSII yields (F_V/F_M) of the leaves are listed in the table (SD in parentheses; **c**)

the analysis confirmed the observations suggested by the data in Fig. 5, indicating that yellow leaves produced $^1O_2$ at higher rates than green leaves, and that the differences in $^1O_2$ production between the leaves with different flavonol contents (but similar chlorophyll contents) were not statistically significant (Table S1).

To verify that a protective effect of flavonols was not masked by other factors in outside grown *B. pendula* leaves, photoinhibition of PSII and PSI was measured from green leaves of *A. thaliana* wild types (Nö-0 and Col-0) and mutants *fls1-2* (Nö-0 background) and *ldox fls1-2* (a cross between the mutants in Nö-0 and Col-0 backgrounds; Fig. 6a). Due to enzymatic blocks in the flavonoid biosynthetic pathway, *fls1-2* is unable to produce flavonols and *ldox fls1-2* lacks both anthocyanins and flavonols (Stracke et al. 2009). The different lines showed small differences in photoinhibition rates but no systematic effect due to the lack of flavonoids could be found (Fig. 6b). Furthermore, flavonols did not affect PSI photoinhibition (Fig. 6c). Fluorescence measurements showed only small differences in UV absorbance between the wild types and the mutants but verified a higher flavonoid level in the Nö-0 wild type than in the flavonoid-less mutants (Fig. 6d).

Discussion

Photosynthetic electron transfer in senescing leaves of *B. pendula*

In the autumn, from the first signs of yellowing, it may take 1–2 months until all leaves of a silver birch (*B. pendula*) tree have fallen. However, during this time individual leaves of the senescing tree remain green until, in seemingly random order, rapid (lasting about 1 week) chlorophyll degradation is initiated (Figs. 1 and S1;

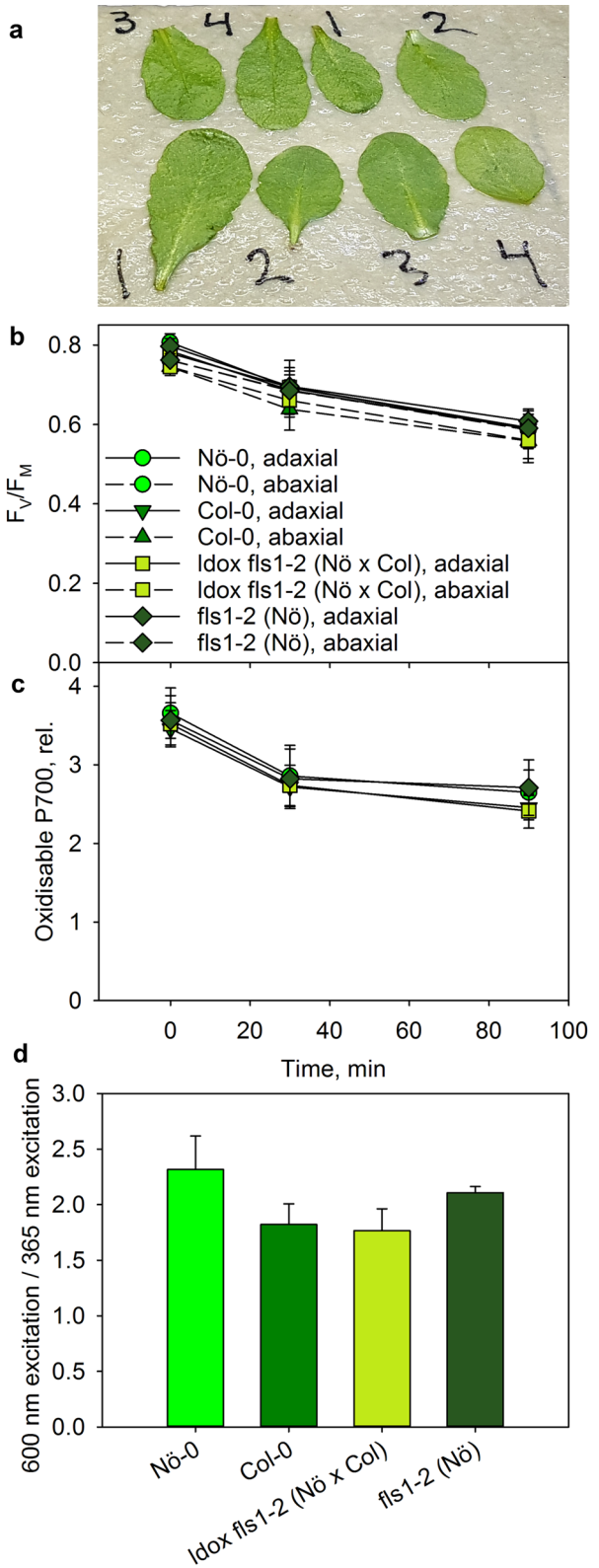

Fig. 6 Leaves of *A. thaliana* Nö-0 (3) and Col-0 (1) wild types and *Idox fls1-2* (4) and *fls1-2* (2) mutants (**a**) were illuminated (PPFD 2000 µmol m^{-2} s^{-1}) at 20 °C, and photoinhibition of PSII (**b**) and PSI (**c**) was measured. F_V/F_M (**b**) was measured from the adaxial and the abaxial side of the leaves. The ratio of chlorophyll fluorescence excited by 600 nm light to chlorophyll fluorescence excited by 365 nm radiation, was measured from the adaxial side (**d**). Error bars show SD from four biological replicates

Mattila et al. 2018). Even in the senescing leaves, the maximum quantum yield of PSII photochemistry stays high until about 90% of chlorophyll is degraded (Fig. 2a), and photochemical quenching of chlorophyll *a* fluorescence is similar in both green and senescing leaves (Fig. 3e). These results show that photosynthetic electron transport remains functional until late senescence, in accordance with previous studies (Keskitalo et al. 2005; Kotakis et al. 2014; Moy et al. 2015). Thus, silver birch keeps photosynthesis ongoing during autumn by two mechanisms. First, senescence of an individual leaf is rapid while most leaves remain fully green, and second, even during degradation of chlorophyll, the remaining photosystems in the leaf retain functionality.

To our knowledge, the fates of the photosynthetic complexes during autumn senescence in *B. pendula* have not been previously reported. We observed an increase in chlorophyll *a* to *b* ratio in the leaves of *B. pendula* during autumnal chlorophyll degradation; the increase was initially quite slow but more remarkable towards abscission (Fig. 2a). Even though the chlorophyll *a* to *b* ratio commonly decreases during autumn senescence in tree species (Lee et al. 2003; Moy et al. 2015), a small increase in chlorophyll *a* to *b* ratio has been previously observed in some senescing trees, e.g. in *Prunus serotina* (black cherry), *A. pensylvanicum* (striped maple) and *Fagus grandifolia* (American beech) (Lee et al. 2003). Because both the F_M yield and the amount of oxidizable P_{700} declined almost linearly with the chlorophyll content of leaves (Fig. 2a), the increasing chlorophyll *a* to *b* ratio suggests that during senescence in *B. pendula*, light harvesting antennae were degraded prior to the photosystems. In *H. vulgare*, an increase in chlorophyll *a* to *b* ratio during leaf senescence was shown to coincide with a decline in the amounts of (some of) the LHCIIs, while the photosystems were assumed to become degraded at rates similar to each other (Krupinska et al. 2012). The present data suggest that LHCI was the main target of degradation in birch during the initial slow phase of an increase in the chlorophyll *a* to *b* ratio. The blue shift in PSI fluorescence at 77 K (Fig. 2c) supports the hypothesis, as the core complex of PSI absorbs at shorter wavelengths than LHCI (Wientjes et al. 2011). Loss of LHCI subunits also agrees with the proportionally higher PSII to PSI ratio in the 77 K spectra (Fig. 2c). The lower in vivo absorption of light at $\lambda > 700$ nm in senescing than in green leaves (Fig. 2b) confirms the loss of some long-wavelength absorbing chlorophylls of LHCI. In addition, FR light oxidized P_{700} more

efficiently in green than in senescing leaves (Fig. 3b, d), further supporting the idea that the antenna size of PSI decreased during senescence. To conclude, the present data suggest that in *B. pendula* degradation first attacks LHCI subunits and during the last phase before abscission, also LHCII is degraded before the photosystems (Figs. 2, 3).

Donation of electrons to P_{700}^+ was slower in senescing than in green leaves (Fig. 3). The findings that (i) P_{700}^+ was re-reduced slowly after an FR treatment, which has little effect on PSII (Fig. 3b), (ii) the maximum quantum yield of PSII photochemistry and photochemical quenching remained high (Fig. 3e) and (iii) the amount of PSII did not seem to decrease faster than that of PSI (Fig. 2), suggest that the limitation causing slow reduction of P_{700}^+ is not PSII but elsewhere in the electron transfer chain. The amount of the cytochrome b6/f complex has been reported to decrease early in both developmental and monocarpic senescence, e.g. in *Avena sativa* (oat) and *Glycine max* (soybean) (Ben-David et al. 1983; Hidema et al. 1991; Guiamét et al. 2002), and also the amount of plastocyanin has been reported to decrease early in monocarpic senescence (Shimakawa et al. 2020). Our data may suggest that these findings might be relevant also in the case of autumn senescence of tree leaves, but the present data do not allow precise localization of the reason for the slow electron donation in *B. pendula*. An increase in the dark-fluorescence level in senescing *B. pendula* leaves was observed in the present study (Fig. 3e). This might be caused by enhanced cyclic electron flow around PSI, as was observed in senescing *Euphorbia dendroides* (tree spurge) (Kotakis et al. 2014) and *H. vulgare* (Catalá et al. 1997), even though increased cyclic electron flow is thought to be associated with the type of senescence where PSII is degraded before PSI (Kotakis et al. 2014; Krieger-Liszkay et al. 2019).

Singlet oxygen and photodamage in senescing leaves

Senescing *B. pendula* leaves produced more $^1O_2$ than green leaves (Fig. 5; Table S1). As evident already from the yellow color of the leaves, the carotenoid to chlorophyll ratio increases during senescence in *B. pendula*. Furthermore, the amount of alpha-tocopherol, a lipid-soluble quencher of $^1O_2$, increases during (early) senescence in *B. alba*; the name refers probably to *B. pubescens* (downy birch) but possibly also to *B. pendula* (García-Plazaola et al. 2003), suggesting that senescing birch leaves indeed need enhanced protection against $^1O_2$.

Development of NPQ decreases $^1O_2$ production (Roach et al. 2012; Dall'Osto et al. 2012), and zeaxanthin, a pigment involved in a form of NPQ, may also directly quench $^1O_2$ (Havaux et al. 2000). Thus, the decreased NPQ capacity of senescing *B. pendula* leaves (Fig. 3c) might have contributed to the higher $^1O_2$ production. NPQ capacity has been shown to decrease during senescence also previously in e.g. *B. pendula* (Sillanpää et al. 2005) and *A. saccharum* (Junker and Ensminger 2015). The F_V/F_M values of green and senescing leaves differed from each other (0.75–0.83 and 0.71–0.82, respectively; calculated based on the data in Fig. 3c), which might suggest that sustained quenching of chlorophyll fluorescence (i.e. quenching that does not relax during a 30 min dark-acclimation time; see Malnoë et al. 2018) would have affected the NPQ values of yellow leaves. However, a plot of the ratio of F_M to chlorophyll content against the chlorophyll content did not show any indication of sustained fluorescence quenching in senescing leaves (Fig. S3).

$^1O_2$ production increases with increasing light intensity (Fufezan et al. 2002; Dall'Osto et al. 2012). Therefore, the diminished absorption of light by senescing leaves (Fig. 2b), which would lead to decreased self-shading, may also contribute to the increased $^1O_2$ production, especially as the decline of chlorophyll in *B. pendula* appears to start from the antenna of PSI that does not produce (much) $^1O_2$ (Hideg and Vass 1995; Cazzaniga et al. 2012).

Photoinhibition of both PSII and PSI proceeded almost three times faster in senescing than in green leaves (Fig. 4). PSII damage increases linearly with light intensity (Tyystjärvi and Aro 1996). Moreover, earlier experiments have shown that the rate of the damaging reaction of photoinhibition of PSII strongly depends on the chlorophyll content of a leaf; photoinhibition increases with decreasing chlorophyll content (Pätsikkä et al. 2002; Serôdio and Campbell 2021). The reason behind this counter-intuitive relationship is that in a dark green leaf, each chloroplast absorbs fewer photons per unit time than in a light green leaf. Furthermore, chlorophyll is not the only photoreceptor of photoinhibition (Hakala et al. 2005; Ohnishi et al. 2005) and, therefore, a high chlorophyll content may also directly screen photoinhibitory light. Thus, the low light absorption by senescing leaves (Fig. 2b) is a possible reason for rapid PSII damage. Senescence in itself does not seem to affect the rate of photoinhibitory damage to PSII in *G. max* (when about 60% of chlorophyll was still present; Guiamét et al. 2002). Growth of *Phaseolus vulgaris* with excess Cu^{2+} (leading to low, ~ 30% of control, chlorophyll content of leaves) also did not enhance damage to PSII when isolated thylakoid membranes were illuminated at a fixed chlorophyll concentration of the suspension (Pätsikkä et al. 2002). The protective effect of high chlorophyll content should not be mixed with the effect of PSII antenna size on photoinhibition, about which there are contrasting results (see Tyystjärvi et al. 1994 Park et al. 1997). The size of PSI antenna that seems to decrease during birch senescence is not likely to determine the rate of PSII photoinhibition. Furthermore, rapid degradation of the

chlorophylls during senescence may be important because undegraded, unbound chlorophyll produces $^1O_2$ with a high quantum yield (Krasnovskii 1977).

It is possible that the increased $^1O_2$ production in senescing leaves contributed to the increased photoinhibition of PSII (Figs. 4, 5). It is known that the repair reactions of PSII are sensitive to $^1O_2$ (Kojima et al. 2009) whereas data speaking both for and against a role for $^1O_2$ in the damaging reaction exist (for a review, see Tyystjärvi 2013). In the present experiments, we did not differentiate between the repair and damage of PSII. Therefore, it is not possible to judge whether the increased $^1O_2$ production of senescing leaves (Fig. 5) directly damaged PSII or slowed down the repair.

In rye (*Secale cereale*), the synthesis of new D1-protein decreases during dark-induced senescence, decreasing the plants' capacity to recover from PSII damage (Kar et al. 1993). On the contrary, even senescing *B. pendula* leaves were able to recover from PSII photoinhibition (Fig. 4c). Anyway, rapid $^1O_2$ production in senescing leaves (Fig. 5) during the high-light treatment may have triggered degradation of chlorophyll (Kar and Feierabend 1984) as, after the subsequent recovery period, fluorescence signals could no longer be measured from about 50% of the senescing leaves. Decreased NPQ has been previously shown to lead to the degradation of chlorophyll in high light (Havaux et al. 2000). It has been proposed that an entire (damaged) chloroplast can be digested, e.g. during senescence (Wada et al. 2008; Martinez et al. 2008), and *B. pendula* might be able to recognize and degrade damaged chloroplasts during autumn senescence. Based on electron microscopy images from senescing *P. tremula* leaves, Keskitalo et al. (2005) proposed that cells with intact chloroplasts and cells with degenerated chloroplasts (gerontoplasts) exist in a single leaf. Indeed, it is well known that senescing leaves do not senesce uniformly, but some areas stay green longer. In the case of *B. pendula*, cells close to veins remain green longer than other areas (Fig. 1; Dodge 1970).

Also PSI was photoinhibited faster in senescing than in green leaves (Fig. 4). Photoinhibition of PSI is caused by excess electron transfer from PSII (Sonoike 1996). However, no acceptor side limitation of PSI was observed in senescing leaves of *B. pendula* (Fig. 3), indicating lack of strong electron pressure at PSI in senescing leaves. The reduction of oxygen to superoxide by PSI has been linked to PSI photoinhibition (Takagi et al. 2016), and senescence has been suggested to enhance the production of superoxide by PSI in *H. vulgare* (Krieger-Liszkay et al. 2015). Furthermore, antioxidative protection may be weak in senescing leaves (Kukavica and Jovanovic 2004). Also $^1O_2$ may damage PSI (Cazzaniga et al. 2012; Takagi et al. 2016) but in green leaves $^1O_2$ is mostly produced by PSII (Hideg and Vass 1995; Cazzaniga et al. 2012), and due to the short lifetime of $^1O_2$ (~2 µs in water; Merkel and Kearns 1972), the damage is expected to occur near the production site (Moan 1990; Mattila et al. 2015). However, PSI might produce $^1O_2$ in senescing leaves.

Flavonols during senescence

It has been suggested that flavonols scavenge $^1O_2$ (Majer et al. 2014). Here, the abundance of flavonols was estimated by measuring differences in the absorbance of UV-A radiation from intact leaves. The method was shown to correlate well (even though not linearly) with the total amounts of flavonols (measured with liquid chromatography) in *B. pendula* leaves (Mattila et al. 2018). The *A. thaliana fls1-2* mutant lacks flavonol synthase activity and consequently most flavonols, and the *ldox fls1-2* double mutant has been shown to contain neither flavonols nor anthocyanins (Stracke et al. 2009). Increased flavonol amounts did not decrease $^1O_2$ production in green or senescing leaves of *B. pendula* (Fig. 5), nor did their absence make the *A. thaliana* mutant leaves more vulnerable to photoinhibition (Fig. 6). Taken together, the data suggest that flavonols do not play a major role in protection against light induced $^1O_2$ production, at least in the present experimental conditions. This is in good accordance with the suggestion that the synthesis of flavonols (which do not contain nitrogen) functions as an energy escape valve during abiotic stress conditions (Hernández and Van Breusegem 2010), and possibly also during autumn senescence. In *B. pendula*, the difference in flavonol levels between the two leaf groups (~1.3 and 1.6) was not huge (even though our previous comparison with a liquid chromatography method suggests that the total amount of flavonols may increase twofold in this case), and, therefore, a small protective effect may have remained undetected.

Conclusions

We present experimental evidence that the remaining photosystems of a senescing silver birch (*B. pendula*) leaf retain full functionality including the repair cycle of PSII functions. However, high light causes a rapid decline in the activities of both photosystems in senescing leaves. In the case of PSII, low chlorophyll content is an obvious reason for rapid photoinhibition. Furthermore, the rate of production of the harmful $^1O_2$ is much faster in a yellow leaf than in a green leaf, and this may contribute to the vulnerability of the photosystems in high light. Flavonols increase during senescence, but these compounds do not seem to affect the susceptibility to high light or the amount of $^1O_2$ in birch leaves.

Supplementary Information The online version contains supplementary material available at https://doi.org/10.1007/s00468-021-02114-x.

Author contribution statement ET and HM designed and supervised the research; HM, PS and TK conducted the experiments; RF provided plant material; KBM provided instrumentation; HM wrote the first draft of the manuscript; ET, KBM, RF, PS and TK contributed in the writing of the final version.

Funding Open access funding provided by University of Turku (UTU) including Turku University Central Hospital. ET was supported by the Academy of Finland (grants 307335 and 333421). HM was supported by the Vilho, Yrjö and Kalle Väisälä Foundation, the Emil Aaltonen Foundation and Doctoral Programme of Molecular Life Sciences (University of Turku). KBM was supported by SustES—Adaptation strategies for sustainable ecosystem services and food security under adverse environmental conditions (CZ.02.1.01/0.0/0.0/16_019/0000797).

Availability of data and materials Raw data are available at Mendeley (https://doi.org/10.17632/dty9cj6gkt.1).

Code availability Not applicable.

Declarations

Conflict of interest None declared.

References

An Y, Feng X, Liu L, Xiong L, Wang L (2016) ALA-induced flavonols accumulation in guard cells is involved in scavenging H2O2 and inhibiting stomatal closure in Arabidopsis cotyledons. Front Plant Sci 7:1713

Ben-David H, Nelson N, Gepstein S (1983) Differential changes in the amount of protein complexes in the chloroplast membrane during senescence of oat and bean leaves. Plant Physiol 73:507–510

Catalá R, Sabater B, Guéra A (1997) Expression of the plastid ndhF gene product in photosynthetic and non-photosynthetic tissues of developing barley seedlings. Plant Cell Physiol 38:1382–1388

Cazzaniga S, Li Z, Niyogi KK, Bassi R, Dall'Osto L, (2012) The Arabidopsis szl1 mutant reveals a critical role of b-carotene in Photosystem I photoprotection. Plant Physiol 159:1745–1758

Cerovic ZG, Masdoumier G, Ghozlen NB, Latouche G (2012) A new optical leaf-clip meter for simultaneous non-destructive assessment of leaf chlorophyll and epidermal flavonoids. Physiol Plant 146:251–260

Cheeseman JM (2009) Seasonal patterns of leaf H2O2 content: reflections of leaf phenology, or environmental stress? Funct Plant Biol 36:721–731

Csepregi K, Hideg É (2017) Phenolic compound diversity explored in the context of photo-oxidative stress protection. Phytochem Anal 29:129–136

Curty C, Engel N (1996) Detection, isolation and structure elucidation of a chlorophyll a catabolite from autumnal senescent leaves of Cercidiphyllum japonicum. Phytochemistry 42:1531–1536

Dall'Osto L, Holt NE, Kaligotla S, Fuciman M, Cazzaniga S, Carbonera D, Frank HA, Alric J, Bassi R, (2012) Zeaxanthin protects plant photosynthesis by modulating chlorophyll triplet yield in specific light-harvesting antenna subunits. T J Biol Chem 287:41820–41834

Dhindsa RJ, Dhindsa PP, Thorpe TA (1981) Leaf senescence: Correlated with increased level of membrane permeability and lipid peroxidation and decreased level of superoxide dismutase and catalase. J Exp Bot 32:93–101

Di Mascio P, Martinez GR, Miyamoto S, Ronsein GE, Medeiros MHG, Cadet J (2019) Singlet molecular oxygen reactions with nucleic acids, lipids, and proteins. Chem Rev 119:2043–2086

Dodge JD (1970) Changes in chloroplast fine structure during the autumnal senescence of Betula leaves. Ann Bot 34:817–824

Franck F, Juneau P, Popovic R (2002) Resolution of the Photosystem I and Photosystem II contributions to chlorophyll fluorescence of intact leaves at room temperature. Biochim Biophys Acta 1556:239–246

Fufezan C, Rutherford AW, Krieger-Liszkay A (2002) Singlet oxygen production in herbicide-treated Photosystem II. FEBS Lett 532:407–410

García-Plazaola JI, Hernández A, Becerril JM (2003) Antioxidant and pigment composition during autumnal leaf senescence in woody deciduous species differing in their ecological traits. Plant Biol 5:557–566

Goulas Y, Cerovic ZG, Cartelat A, Moya I (2004) Dualex: A new instrument for field measurements of epidermal UV-absorbance by chlorophyll fluorescence. Appl Opt 43:4488–4496

Guiamét J, Tyystjärvi E, Tyystjärvi T, John I, Kairavuo M, Pichersky E, Noodén LD (2002) Photoinhibition and loss of photosystem II reaction centre proteins during senescence of soybean leaves. Enhancement of photoinhibition by the 'stay-green' mutation cytG. Physiol Plantarum 115:468–478

Hakala M, Tuominen I, Keränen M, Tyystjärvi T, Tyystjärvi E (2005) Evidence for the role of the oxygen-evolving manganese complex in photoinhibition of photosystem II. Biochim Biophys Acta 1706:68–80

Havaux M, Bonfils JP, Lütz C, Niyogi KK (2000) photodamage of the photosynthetic apparatus and its dependence on the leaf developmental stage in the npq1 arabidopsis mutant deficient in the xanthophyll cycle enzyme violaxanthin de-epoxidase. Plant Physiol 124:273–284

Hernández I, Van Breusegem F (2010) Opinion on the possible role of flavonoids as energy escape valves: Novel tools for nature's Swiss army knife? Plant Sci 179:297–301

Hideg É, Vass I (1995) Singlet oxygen is not produced in photosystem I under photoinhibitory conditions. Photochem Photobiol 62:949–952

Hidema J, Makino A, Mae T, Ojima K (1991) Photosynthetic characteristics of rice leaves aged under different irradiances from full expansion through senescence. Plant Physiol 97:1287–1293

Hoch WA, Singsaas EL, McCown BH (2003) Resorption protection. Anthocyanins facilitate nutrient recovery in autumn by shielding leaves from potentially damaging light levels. Plant Physiol 133:1296–1305

Hogewoning SW, Wientjes E, Douwstra P, Trouwborst G, van Ieperen W, Croce R, Harbinson J (2012) Photosynthetic quantum yield dynamics: From photosystems to leaves. Plant Cell 24:1921–1935

Hörtensteiner S (2004) The loss of green color during chlorophyll degradation—a prerequisite to prevent cell death? Planta 219:191–194
Hung KT, Kao CH (2005) Hydrogen peroxide is necessary for abscisic acid-induced senescence of rice leaves. J Plant Physiol 161:1347–1357
Hynynen J, Niemistö P, Viherä-Aarnio A, Brunner A, Hein S, Velling P (2010) Silviculture of birch (*Betula pendula* Roth and *Betula pubescens* Ehrh.) in northern Europe. Forestry 83:103–119
Idle PB, Proctor CW (1983) An integrating sphere leaf chamber. Plant Cell Environ 6:437–439
Jajić I, Sarna T, Szewczyk G, Strzałka K (2015) Changes in production of reactive oxygen species in illuminated thylakoids isolated during development and senescence of barley. J Plant Physiol 184:49–56
Junker LV, Ensminger I (2015) Relationship between leaf optical properties, chlorophyll fluorescence and pigment changes in senescing Acer saccharum leaves. Tree Physiol 36:694–711
Kar M, Feierabend J (1984) Metabolism of activated oxygen in detached wheat and rye leaves and its relevance to the initiation of senescence. Planta 160:385–391
Kar M, Streb P, Hertwig B, Feierabend J (1993) Sensitivity to photodamage increases during senescence in excised leaves. J Plant Physiol 141:538–544
Kashiyama Y, Tamiaki H (2014) Risk management by organisms of the phototoxicity of chlorophylls. Chem Lett 43:148–156
Keskitalo J, Bergquist G, Gardeström P, Jansson S (2005) A cellular timetable of autumn senescence. Plant Physiol 139:1635–1648
Kojima K, Oshita M, Nanjo Y, Kasai K, Tozawa Y, Hayashi H, Nishiyama Y (2009) Oxidation of elongation factor G inhibits the synthesis of the D1 protein of photosystem II. Mol Microbiol 65:936–947
Kotakis C, Kyzeridou A, Manetas Y (2014) Photosynthetic electron flow during leaf senescence: Evidence for a preferential maintenance of photosystem I activity and increased cyclic electron flow. Photosynthetica 52:413–420
Kramer DM, Johnson G, Kiirats O, Edwards GE (2004) New flux parameters for the determination of QA redox state and excitation fluxes. Photosynth Res 79:209–218
Krasnovskii AA Jr (1977) Photoluminescence of singlet oxygen in solutions of the chlorophylls and pheophytins. Biofizika 22:927–928
Kräutler B, Jaun B, Bortlik KH, Schellenberg M, Matile P (1991) On the enigma of chlorophyll degradation: the constitution of a secoporphinoid catabolite. Angew Chem Int Ed Engl 30:1315–1318
Krieger-Liszkay A, Krupinska K, Shimakawa G (2019) The impact of photosynthesis on initiation of leaf senescence. Physiol Plantarum 166:148–164
Krieger-Liszkay A, Trösch M, Krupinska K (2015) Generation of reactive oxygen species in thylakoids from senescing flag leaves of the barley varieties Lomerit and Carina. Planta 241:1497–1508
Krupinska K, Mulisch M, Hollmann J, Tokarz K, Zschiesche W, Kage H, Humbeck K, Bilger W (2012) An alternative strategy of dismantling of the chloroplasts during leaf senescence observed in a high-yield variety of barley. Physiol Plantarum 144:189–200
Kuai B, Chen J, Hörtensteiner S (2018) The biochemistry and molecular biology of chlorophyll breakdown. J Exp Bot 69:751–767
Kukavica B, Jovanovic SV (2004) Senescence-related changes in the antioxidant status of ginkgo and birch leaves during autumn yellowing. Physiol Plant 122:321–327
Lee DW, O'Keefe J, Holbrook NM, Feild TS (2003) Pigment dynamics and autumn leaf senescence in a New England deciduous forest, eastern USA. Ecol Res 18:677–694
Leshem YY (1988) Plant senescence processes and free radicals. Free Radic Biol Med 5:39–49
Majer P, Neugart S, Krumbein A, Schreiner M, Hideg É (2014) Singlet oxygen scavenging by leaf flavonoids contributes to sunlight acclimation in Tilia platyphyllos. Environ Exper Bot 100:1–9
Malnoë A, Schultink A, Shahrasbi S, Rumeau D, Havaux M, Niyogi KK (2018) The plastid lipocalin LCNP is required for sustained photoprotective energy dissipation in Arabidopsis. Plant Cell 30:196–208
Martinez DE, Costa ML, Gomez FM, Otegui MS, Guiamet JJ (2008) 'Senescence-associated vacuoles' are involved in the degradation of chloroplast proteins in tobacco leaves. Plant J 56:196–206
Matile P, Ginsburg S, Schellenberg M, Thomas H (1988) Catabolites of chlorophyll in senescing barley leaves are localized in the vacuoles of mesophyll cells. Proc Natl Acad Sci USA 85:9529–9532
Mattila H, Khorobrykh S, Hakala-Yatkin M, Havurinne V, Kuusisto I, Antal T, Tyystjärvi T, Tyystjärvi E (2020) Action spectrum of the redox state of the plastoquinone pool defines its function in plant acclimation. Plant J 104:1088–1104
Mattila H, Khorobrykh S, Havurinne V, Tyystjärvi E (2015) Reactive oxygen species: Reactions and detection from photosynthetic tissues. J Photochem Photobiol B 152:176–214
Mattila H, Valev D, Havurinne V, Khorobrykh S, Virtanen O, Antinluoma M, Mishra KB, Tyystjärvi E (2018) Degradation of chlorophyll and synthesis of flavonols during autumn senescence—the story told by individual leaves. Ann Bot PLANTS. https://doi.org/10.1093/aobpla/ply028
Mayta ML, Lodeyro AF, Guiamet JJ, Tognetti VB, Melzer M, Hajirezaei MR, Carrillo N (2018) Expression of a plastid-targeted flavodoxin decreases chloroplast reactive oxygen species accumulation and delays senescence in aging tobacco leaves. Front Plant Sci 9:1039
Mazor Y, Borovikova A, Nelson N (2015) The structure of plant photosystem I super-complex at 2.8 Å resolution. eLife 4:e07433
Merkel PB, Kearns DR (1972) Radiationless decay of singlet molecular oxygen in solution. An experimental and theoretical study of electronic-to-vibrational energy transfer. J Am Chem Soc 94:7244–7253
Moan J (1990) On the diffusion length of singlet oxygen in cells and tissues. J Photochem Photobiol B 6:343–347
Morales LO, Tegelberg R, Brosché M, Keinänen M, Lindfors A, Aphalo PJ (2010) Effects of solar UV-A and UV-B radiation on gene expression and phenolic accumulation in Betula pendula leaves. Tree Physiol 30:923–934
Moy A, Le S, Verhoeven A (2015) Different strategies for photoprotection during autumn senescence in maple and oak. Physiol Plantarum 155:205–216
Muhlemann JK, Younts TLB, Muday GK (2018) Flavonols control pollen tube growth and integrity by regulating ROS homeostasis during high temperature stress. Proc Natl Acad Sci USA 115:E11188–E11197
Ohnishi N, Allakhverdiev SI, Takahashi S, Higashi S, Watanabe M, Nishiyama Y, Murata N (2005) Two-step mechanism of photodamage to Photosystem II: Step 1 occurs at the oxygen-evolving complex and step 2 occurs at the photochemical reaction center. Biochemistry 44:8494–8499
Paaso U, Keski-Saari S, Keinänen M, Karvinen H, Silfver T, Rousi M, Mikola J (2017) Intrapopulation genotypic variation of foliar secondary chemistry during leaf senescence and litter decomposition in silver birch (Betula pendula). Front Plant Sci 8:1074
Park Y-I, Chow WS, Anderson JM (1997) Antenna size dependency of photoinactivation of photosystem II in light-acclimated pea leaves. Plant Physiol 115:151–157
Pätsikkä E, Aro EM, Tyystjärvi E (1998) Increase in the quantum yield of photoinhibition contributes to copper toxicity in vivo. Plant Physiol 117:619–627
Pätsikkä E, Kairavuo M, Šeršen F, Aro EM, Tyystjärvi E (2002) Excess copper predisposes photosystem II to photoinhibition

in vivo by outcompeting iron and causing decrease in leaf chlorophyll. Plant Physiol 129:1359–1367

Porra RJ, Thompson WA, Kriedemann PE (1989) Determination of accurate extinction coefficients and simultaneous equations for assaying chlorophylls a and b extracted with four different solvents: verification of the concentration of chlorophyll standards by atomic absorption spectroscopy. Biochim Biophys Acta 975:384–394

Procházková D, Wilhelmová N (2007) Leaf senescence and activities of the antioxidant enzymes. Biol Plant 51:401–406

Przybyla D, Gobel C, Imboden A, Feussner I, Hamberg M, Apel K (2008) Enzymatic, but not non-enzymatic $^1O_2$-mediated peroxidation of polyunsaturated fatty acids forms part of the EXECUTER1-dependent stress response program in the *flu* mutant of *Arabidopsis thaliana*. Plant J 54:236–248

Ragás X, Jiménez-Banzo A, Sánchez-García D, Batllori X, Nonell S (2009) Singlet oxygen photosensitisation by the fluorescent probe Singlet Oxygen Sensor Green®. Chem Commun 20:2920–2922

Roach T, Krieger-Liszkay A (2012) The role of the PsbS protein in the protection of photosystems I and II against high light in Arabidopsis thaliana. Biochim Biophys Acta 1817:2158–2165

Schreiber U, Klughammer C (2016) Analysis of Photosystem I donor and acceptor sides with a new type of online-deconvoluting kinetic LED-array spectrophotometer. Plant Cell Physiol 57:1454–1467

Serôdio J, Campbell DA (2021) Photoinhibition in optically thick samples: effects of light attenuation on chlorophyll fluorescence-based parameters. J Theor Biol 513:110580

Shi D, Wei X, Chen G, Xu Y (2012) Changes in photosynthetic characteristics and antioxidative protection in male and female ginkgo during natural senescence. J Amer Soc Hort Sci 137:349–360

Shimakawa G, Roach T, Krieger-Liszkay A (2020) Changes in photosynthetic electron transport during leaf senescence in two barley varieties grown in contrasting growth regimes. Plant Cell Physiol, pcaa114

Sillanpää M, Kontunen-Soppela S, Luomala EM, Sutinen S, Kangasjärvi J, Häggman H, Vapaavuori E (2005) Expression of senescence-associated genes in the leaves of silver birch (Betula pendula). Tree Physiol 25:1161–1172

Sitko K, Rusinowski S, Pogrzeba M, Daszkowska-Golec A, Gieroń Ż, Kalaji HM, Małkowski E (2019) Development and aging of photosynthetic apparatus of *Vitis vinifera* L. during growing season. Photosynthetica 57:1–8

Sonoike K (1996) Photoinhibition of photosystem I: its physiological significance in the chilling sensitivity of plants. Plant Cell Physiol 37:239–247

Springer A, Acker G, Bartsch S, Bauerschmitt H, Reinbothe S, Reinbothe C (2015) Differences in gene expression between natural and artificially induced leaf senescence in barley. J Plant Physiol 176:180–191

Stark S, Väisänen M, Ylänne H, Julkunen-Tiitto R, Martz F (2015) Decreased phenolic defense in dwarf birch (Betula nana) after warming in subarctic tundra. Polar Biol 38:1993–2005

Stracke R, De Vos RCH, Bartelniewoehner L, Ishihara H, Sagasser M, Martens S, Weisshaar B (2009) Metabolomic and genetic analyses of flavonol synthesis in Arabidopsis thaliana support the in vivo involvement of leucoanthocyanidin dioxygenase. Planta 229:427–445

Takagi D, Takumi S, Hashiguchi M, Sejima T, Miyake C (2016) Superoxide and singlet oxygen produced within the thylakoid membranes both cause Photosystem I. photoinhibition. Plant Physiol 171:1626–1634

Tanaka R, Hirashima M, Satoh S, Tanaka A (2003) The Arabidopsis-accelerated cell death gene ACD1 is involved in oxygenation of pheophorbide a: inhibition of the pheophorbide a oxygenase activity does not lead to the "stay-green" phenotype in Arabidopsis. Plant Cell Physiol 44:1266–1274

Taulavuori K, Pihlajaniemi H, Huttunen S, Taulavuori E (2011) Reddish spring colouring of deciduous leaves: A sign of ecotype? Trees 25:231–236

Tyystjärvi E (2013) Photoinhibition of Photosystem II. Int Rev Cell Mol Biol 300:343–303

Tyystjärvi E, Kettunen R, Aro E-M (1994) The rate constant of photoinhibition in vitro is independent of the antenna size of Photosystem II but depends on temperature. Biochim Biophys Acta 1186:177–185

Tyystjärvi E, Aro EM (1996) The rate constant of photoinhibition, measured in lincomycin-treated leaves, is directly proportional to light intensity. Proc Natl Acad Sci USA 93:2213–2218

Wada S, Ishida H, Izumi M, Yoshimoto K, Ohsumi Y, Mae T, Makino A (2008) Autophagy plays a role in chloroplast degradation during senescence in individually darkened leaves. Plant Physiol 149:885–893

Wang F, Liu J, Zhou L, Pan G, Li Z, Zaidi SHR, Cheng F (2016) Senescence-specific change in ROS scavenging enzyme activities and regulation of various SOD isozymes to ROS levels in psf mutant rice leaves. Plant Physiol Biochem 109:248–261

Watkins JM, Chapman JM, Muday GK (2017) Abscisic acid-induced reactive oxygen species are modulated by flavonols to control stomata aperture. Plant Physiol 175:1807–1825

Wei X, Su X, Cao P, Liu X, Chang W, Li M, Zhang X, Liu Z (2016) Structure of spinach photosystem II-LHCII supercomplex at 3.2 Å resolution. Nature 534:69–74

Weis E (1985) Chlorophyll fluorescence at 77 K in intact leaves: Characterization of a technique to eliminate artifacts related to self-absorption. Photosynth Res 6:73–86

Wientjes E, van Stokkum IHM, van Amerongen H, Croce R (2011) The role of the individual Lhcas in photosystem I excitation energy trapping. Biophys J 101:745–754